High-order Curvilinear Finite Element Scheme for Nonlocal Transport in Lagrangian Hydrodynamics

Milan Holec

CELIA, University of Bordeaux,
33405 Talence, France
(milan.holec@u-bordeaux.fr)

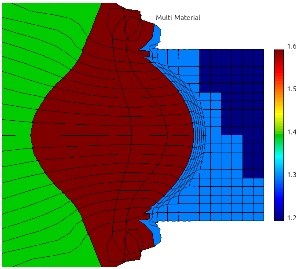

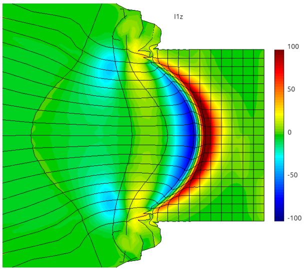

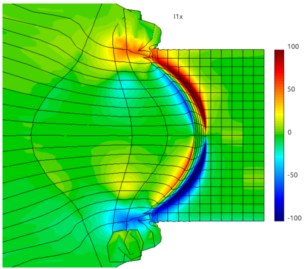

MULTIMAT
SANTA FE, NM, USA
SEPTEMBER 18-22, 2017

Hydrodynamic model of plasma

Boltzmann transport equation

$$\frac{\partial f}{\partial t} + \boldsymbol{v} \cdot \nabla_x f + \frac{q_e}{m_e}\left(\boldsymbol{E} + \frac{\boldsymbol{v}}{c} \times \boldsymbol{B}\right) \cdot \nabla_{\boldsymbol{v}} f = C(f, f)$$

Fluid equations

$$\begin{aligned}
\frac{\mathrm{d}\rho}{\mathrm{d}t} &= -\rho \nabla_{\boldsymbol{x}} \cdot \boldsymbol{U} \\
\rho \frac{\mathrm{d}\boldsymbol{U}}{\mathrm{d}t} &= \nabla_{\boldsymbol{x}} \cdot \sigma \\
\rho \frac{\mathrm{d}\varepsilon}{\mathrm{d}t} &= \sigma : \nabla_{\boldsymbol{x}} \boldsymbol{U} - \nabla_{\boldsymbol{x}} \cdot \boldsymbol{q}
\end{aligned}$$

Microscopic closure

$$\begin{aligned}
\sigma &= -\rho \int (\boldsymbol{v} - \boldsymbol{U}) \otimes (\boldsymbol{v} - \boldsymbol{U})\, f \, \mathrm{d}\boldsymbol{v}^3 \approx -\mathbf{I}p + \tilde{\sigma}(\nabla \boldsymbol{U}) \\
\boldsymbol{q} &= \frac{\rho}{2} \int |\boldsymbol{v} - \boldsymbol{U}|^2 (\boldsymbol{v} - \boldsymbol{U})\, f \, \mathrm{d}\boldsymbol{v}^3 \approx 2\pi\rho \int_{4\pi} \boldsymbol{n} \int_0^\infty |\boldsymbol{v}|^5 f \, \mathrm{d}|\boldsymbol{v}| \, \mathrm{d}\boldsymbol{n} \approx -\kappa(T^{2.5}) \nabla T
\end{aligned}$$

Nonlocal vs. diffusive transport models

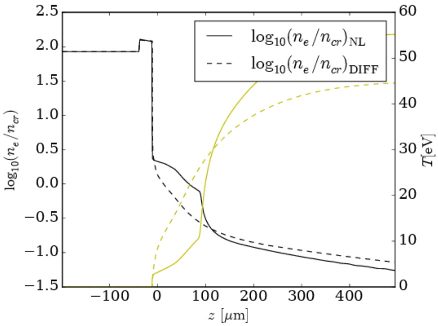

pre-pulse 10^{12} W/cm^2 (10^{22} W/cm^2)

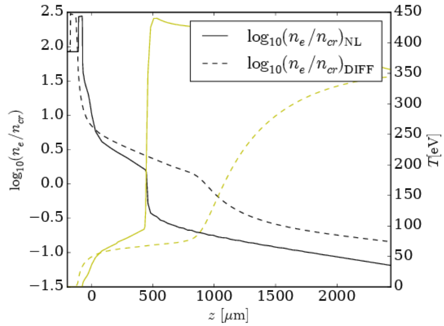

pre-pulse 10^{14} W/cm^2 (10^{24} W/cm^2)

$$\frac{1}{|\boldsymbol{v}|}\frac{\partial f^e}{\partial t} + \boldsymbol{n}\cdot\nabla_x f^e + \frac{q_e}{m_e|\boldsymbol{v}|}\boldsymbol{E}\cdot\nabla_{\boldsymbol{v}} f^e = \frac{f_{MB}(|\boldsymbol{v}|, T_e) - f^e}{\lambda},$$

Chapman-Enskog approximation in small parameter λ

$$f^e = f_0 + \lambda f_1 + O(\lambda^2) \approx f_{MB}(|\boldsymbol{v}|, T_e) - f_{MB}(|\boldsymbol{v}|, T_e) g(\bar{Z})\left(\frac{|\boldsymbol{v}|^2}{2v_{T_e}^2} - 4\right)\boldsymbol{n}\cdot\frac{\lambda\nabla T_e}{T_e}$$

$$\frac{\lambda f_1}{f_0} = 0.25\left(\frac{|\boldsymbol{v}|^2}{2v_{T_e}^2} - 4\right)\boldsymbol{n}\cdot\frac{\lambda(|\boldsymbol{v}|)\nabla T_e}{T_e} < 0.1 \quad \longrightarrow \quad \mathrm{Kn}^e = \frac{\lambda\nabla T_e}{T_e} < 7.5\times 10^{-4}$$

Nonlocal transport in hydrodynamics review

Kinetic Fokker-Planck-Landau equation

$$\frac{1}{|\boldsymbol{v}|}\frac{\partial f}{\partial t} + \boldsymbol{n}\cdot\nabla_x f + \frac{q_e}{m_e}\left(\frac{\boldsymbol{E}}{|\boldsymbol{v}|} + \frac{\boldsymbol{n}}{c}\times\boldsymbol{B}\right)\cdot\nabla_{\boldsymbol{v}} f = \frac{1}{\lambda}\nabla_{\boldsymbol{v}}\cdot\int \frac{|\boldsymbol{v}-\boldsymbol{v}'|^2\mathbf{I} - (\boldsymbol{v}-\boldsymbol{v}')\otimes\boldsymbol{v}-\boldsymbol{v}')}{|\boldsymbol{v}-\boldsymbol{v}'|^3}\left(\nabla_{\boldsymbol{v}} f(\boldsymbol{v})f(\boldsymbol{v}') - f(\boldsymbol{v})\nabla_{\boldsymbol{v}} f(\boldsymbol{v}')\right)\mathrm{d}\boldsymbol{v}'$$

Computationally efficient simplifications:

- SH flux electron heat conduction (Chapman-Enskog expansion based local approximation [Spitzer and Harm, PR 89, 977 (1953)])
- LMV delocalized flux (1D spatial convolution of SH flux [Luciani, Mora, and Virmont, PRL 51, 1664 (1983).], further improved in spectral space [Epperlein and Short, PF B 4, 2211 (1992)]
- SNB multi-dimensional extension (linear transport equation of SH flux [Schurtz, Nicolai, and Busquet, PoP 7, 4238 (2000)])
- M1 model (finite transport equation moments hierarchy based on angular entropy minimization closure [Sorbo et al, PoP 22, 082706 (2015)])
- BGK transport equation (1D analytic solution [Manheimer, Colombant, and Goncharov, PoP 15, 083103 (2008)])

Kinetic Nonlocal Transport Hydrodynamic (NTH) equation

$$\boldsymbol{n}\cdot\nabla_x f + \frac{q_e}{m_e|\boldsymbol{v}|}\left(\boldsymbol{E}\cdot\boldsymbol{n}\frac{\partial}{\partial|\boldsymbol{v}|}f + \left(\frac{\boldsymbol{E}}{|\boldsymbol{v}|} + \frac{\boldsymbol{n}}{c}\times\boldsymbol{B}\right)\cdot\nabla_{\boldsymbol{n}} f\right) = \frac{f_{MB}(|\boldsymbol{v}|, T_e) - f}{\lambda_{ei}} + \frac{|\boldsymbol{v}|}{\lambda_{ee}}\frac{\partial}{\partial|\boldsymbol{v}|}\left(\frac{v_T^2}{|\boldsymbol{v}|}\frac{\partial}{\partial|\boldsymbol{v}|} + 1\right)(f - f_0)$$

Radiation transport equation

$$\boldsymbol{n}\cdot\nabla_x I = \frac{I_P - I}{\lambda} + \frac{I_0 - I}{\tilde{\lambda}}, \qquad I_0 = \frac{1}{4\pi}\int_{4\pi} I\,\mathrm{d}\boldsymbol{n}, \qquad \boldsymbol{q} = \int_{4\pi}\boldsymbol{n} I\,\mathrm{d}\boldsymbol{n}$$

Planar geometry - transport equation

$$\cos(\Phi)\frac{\partial I}{\partial z} = S_T T_e - kI\,,$$

$$I(t,z,\Phi) = (\boldsymbol{\omega}_\Phi \otimes \boldsymbol{\psi}_z)^T \cdot \boldsymbol{I}^{n+1},\ T_e(t,z) = \boldsymbol{\phi}_z^T \cdot \boldsymbol{T}_e^{n+1}$$

Composition of the multi-dimensional interpolation based on *outerproduct* $\otimes$

$$\boldsymbol{\omega}_\Phi = [\omega_1(\Phi),..,\omega_{M_\Phi}(\Phi)]^T, \boldsymbol{\psi}_z = [\psi_1(z),..,\psi_{N_f}(z)]^T,\ \boldsymbol{\phi}_z = [\phi_1(z),..,\phi_{N_e}(z)]^T$$

$$\int_{\Omega_\Phi}\int_{\Omega_z} (\boldsymbol{\omega}_\Phi \otimes \boldsymbol{\psi}_z) \otimes \left[\cos(\Phi)\left(\boldsymbol{\omega}_\Phi \otimes \frac{\partial \boldsymbol{\psi}_z}{\partial z}\right)^T \cdot \boldsymbol{I}^{n+1} + k\,(\boldsymbol{\omega}_\Phi \otimes \boldsymbol{\psi}_z)^T \cdot \boldsymbol{I}^{n+1} - (\boldsymbol{\omega}_\Phi \otimes \boldsymbol{\phi}_z)^T \cdot \mathbf{S}_T \cdot \boldsymbol{T_e}^{n+1}\right] \mathrm{d}\Omega_z \sin(\Phi)\,\mathrm{d}\Phi =$$

$$\int_{\Omega_\Phi}\int_{\Gamma_{\boldsymbol{n}\cdot\boldsymbol{n}_\Gamma<0}} (\boldsymbol{\omega}_\Phi \otimes \boldsymbol{\psi}_z) \otimes \left[(\boldsymbol{\omega}_\Phi \otimes \boldsymbol{\psi}_z)^T \cdot \boldsymbol{I}^{n+1} - \left(\boldsymbol{\omega}_\Phi \otimes \tilde{\boldsymbol{\psi}}_z\right)^T \cdot \tilde{\boldsymbol{I}}\right] (\cos(\Phi)\boldsymbol{n}_\Gamma^z)\ \mathrm{d}\Gamma_z \sin(\Phi)\,\mathrm{d}\Phi$$

Discrete DG transport equation - transport operator inversion $\boldsymbol{I}^{n+1} = \mathbf{A}\cdot \boldsymbol{T}_e^{n+1} + \boldsymbol{b}(\tilde{\boldsymbol{I}})$

$$\mathbf{D}\cdot \boldsymbol{I}^{n+1} + k\mathbf{M}\cdot \boldsymbol{I}^{n+1} - \mathbf{B}\cdot \boldsymbol{I}^{n+1} = \mathbf{S}\cdot \boldsymbol{T_e}^{n+1} - \tilde{\mathbf{B}}\cdot \tilde{\boldsymbol{I}}$$

Exact steady state "given direction" transport

$$\cos(\Phi_0)\,\frac{\mathrm{d}I(z,\Phi_0)}{\mathrm{d}z} = k\left(\sin(\pi z) - I(z,\Phi_0)\right)$$

Three different values of $k = 10^{-4}, 1, 10^{4}$, which corresponds to free-streaming, nonlocal, and diffusive transport ($\Phi_0 = \pi/4$).

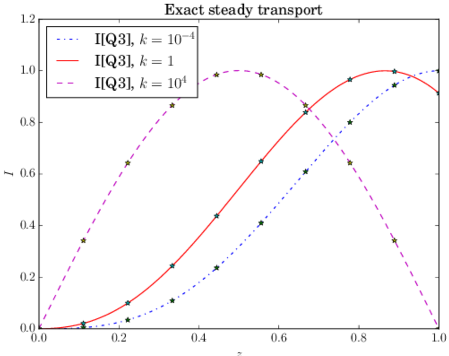

element	cells	$E_{L1}^{k=10^{-4}}$	$q_{L1}^{k=10^{-4}}$	$E_{L1}^{k=1}$	$q_{L1}^{k=1}$	$E_{L1}^{k=10^4}$	$q_{L1}^{k=10^4}$
I[Q1]	10	2.7e-07		2.3e-03		8.3e-03	
I[Q1]	20	4.9e-08	2.5	4.3e-04	2.4	1.6e-03	2.4
I[Q1]	40	1.2e-08	2.0	1.1e-04	2.0	3.7e-04	2.1
I[Q1]	80	2.9e-09	2.0	2.6e-05	2.0	9.0e-05	2.1
I[Q2]	10	4.6e-09		4.1e-05		3.5e-07	
I[Q2]	20	4.1e-10	3.5	3.5e-06	3.5	5.2e-08	2.8
I[Q2]	40	4.5e-11	3.2	4.0e-07	3.2	1.2e-08	2.1
I[Q2]	80	5.4e-12	3.1	4.7e-08	3.1	2.8e-09	2.1
I[Q3]	10	7.3e-11		2.6e-07		2.3e-06	
I[Q3]	20	2.8e-12	4.7	8.4e-09	5.0	1.0e-07	4.5
I[Q3]	40	1.5e-13	4.2	4.3e-10	4.3	5.6e-09	4.2
I[Q3]	80	8.9e-15	4.1	2.4e-11	4.1	3.3e-10	4.1

It is worth mentioning that the method works well also in diffusive limit $k = 10^4$ ($Kn \approx 10^{-4}$).

Exact steady state "full" transport

Model steady equation

$$\cos(\Phi)\,\frac{\mathrm{d}I(z,\Phi)}{\mathrm{d}z} = k\left(S(z) - I(z,\Phi)\right)$$

Energy density flux

$$\boldsymbol{q}(z) = 2\pi\int_0^{\pi}\cos(\Phi)\,I(z,\Phi)\,\sin(\Phi)\,\mathrm{d}\Phi$$

Divergence of energy density flux

$$\nabla\cdot\boldsymbol{q}(z) = 2\pi\int_0^{\pi}\cos(\Phi)\,\frac{\partial I(z,\Phi)}{\partial z}\,\sin(\Phi)\,\mathrm{d}\Phi$$

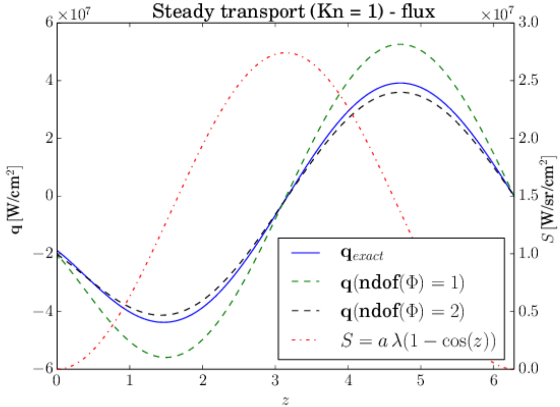

Relative L1 error convergence in polar angle Φ of $\nabla\cdot\boldsymbol{q}$

transport regime	Kn=λ/L — ndof(Φ)	1	2	3	4	5	20	40
transparent/ballistic	100.0	1.5e-01	4.1e-01	9.5e-02	2.4e-01	7.1e-02	5.1e-02	2.2e-02
nonlocal/highly anisotropic	10.0	2.0e-01	3.7e-01	1.1e-01	2.0e-01	7.8e-02	1.3e-02	1.1e-03
nonlocal/anisotropic	1.0	3.5e-01	8.8e-02	2.6e-02	1.1e-02	2.7e-03	1.1e-05	9.6e-07
nonlocal/almost isotropic	0.1	1.5e-01	9.6e-03	4.8e-03	3.3e-3	6.9e-04	5.7e-07	4.6e-07
diffusive/isotropic	0.01	1.4e-01	1.0e-02	5.9e-03	4.5e-03	2.0e-03	2.9e-05	2.9e-05

Planar geometry - transport equation

$$\cos(\Phi)\frac{\partial I}{\partial z} = S_T T_e - (k + \cos(\Phi) E_z) I + \sigma I_0\,, \quad I_0 = \frac{1}{2}\int_{\Omega_\Phi} I \sin(\Phi)\, \mathrm{d}\Phi$$

$$I(t,z,\Phi) = (\boldsymbol{\omega}_\Phi \otimes \boldsymbol{\psi}_z)^T \cdot \boldsymbol{I}^{n+1},\ T_e(t,z) = \boldsymbol{\phi}_z^T \cdot \boldsymbol{T}_e^{n+1}$$

Composition of the multi-dimensional interpolation based on *outerproduct*$\otimes$

$$\boldsymbol{\omega}_\Phi = [\omega_1(\Phi), .., \omega_{M_\Phi}(\Phi)]^T, \boldsymbol{\psi}_z = [\psi_1(z), .., \psi_{N_f}(z)]^T,\ \boldsymbol{\phi}_z = [\phi_1(z), .., \phi_{N_e}(z)]^T$$

$$\int_{\Omega_\Phi}\int_{\Omega_z} (\boldsymbol{\omega}_\Phi \otimes \boldsymbol{\psi}_z) \otimes \left[\cos(\Phi)\left(\boldsymbol{\omega}_\Phi \otimes \frac{\partial \boldsymbol{\psi}_z}{\partial z}\right)^T \cdot \boldsymbol{I}^{n+1} + (k + \cos(\Phi) E_z)(\boldsymbol{\omega}_\Phi \otimes \boldsymbol{\psi}_z)^T \cdot \boldsymbol{I}^{n+1} - \frac{\sigma}{2}\int_{\Omega_\Phi} \boldsymbol{\omega}_\Phi^T \sin(\Phi) \mathrm{d}\Phi \otimes \boldsymbol{\psi}_z^T \cdot \boldsymbol{I}^{n+1} \right.$$

$$\left. - (\boldsymbol{\omega}_\Phi \otimes \boldsymbol{\phi}_z)^T \cdot \mathbf{S}_T \cdot \boldsymbol{T_e}^{n+1}\right] \mathrm{d}\Omega_z \sin(\Phi)\, \mathrm{d}\Phi =$$

$$\int_{\Omega_\Phi}\int_{\Gamma_{\boldsymbol{n}\cdot\boldsymbol{n}_\Gamma<0}} (\boldsymbol{\omega}_\Phi \otimes \boldsymbol{\psi}_z) \otimes \left[(\boldsymbol{\omega}_\Phi \otimes \boldsymbol{\psi}_z)^T \cdot \boldsymbol{I}^{n+1} - \left(\boldsymbol{\omega}_\Phi \otimes \tilde{\boldsymbol{\psi}}_z\right)^T \cdot \tilde{\boldsymbol{I}}\right] (\cos(\Phi) \boldsymbol{n}_\Gamma^z)\ \mathrm{d}\Gamma_z \sin(\Phi)\, \mathrm{d}\Phi$$

Discrete DG transport equation - transport operator inversion $\boldsymbol{I}^{n+1} = \mathbf{A} \cdot \boldsymbol{T}_e^{n+1} + \boldsymbol{b}(\tilde{\boldsymbol{I}})$

$$\mathbf{D} \cdot \boldsymbol{I}^{n+1} + ((k+\sigma)\mathbf{M} + E_z \mathbf{M}_{\cos(\Phi)} - \sigma \mathbf{MI}) \cdot \boldsymbol{I}^{n+1} - \mathbf{B} \cdot \boldsymbol{I}^{n+1} = \mathbf{S} \cdot \boldsymbol{T_e}^{n+1} - \tilde{\mathbf{B}} \cdot \tilde{\boldsymbol{I}}$$

Planar geometry - energy equation equipped with the nonlocal transport

$$a\frac{\mathrm{d}T_e}{\mathrm{d}t} + G_{ei}(T_e - T_i) + \int_{4\pi} \cos(\Phi)\frac{\partial I}{\partial z}\sin(\Phi)\,\mathrm{d}\Phi\,\mathrm{d}\Theta = P_e$$

$$I(t,z,\Phi) = (\boldsymbol{\omega}_\Phi \otimes \boldsymbol{\psi}_z)^T \cdot \boldsymbol{I}^{n+1},\; T_e(t,z) = \boldsymbol{\phi}_z^T \cdot \boldsymbol{T}_e^{n+1},\; T_i(t,z) = \tilde{\boldsymbol{\phi}}_z{}^T \cdot \boldsymbol{T}_i^{n+1}$$

$$\int_{\Omega_z} \boldsymbol{\phi}_z \otimes \left[a\,\boldsymbol{\phi}_z^T \cdot \frac{\boldsymbol{T}_e^{n+1} - \boldsymbol{T}_e^n}{\Delta t} + G_{ei}\left(\boldsymbol{\phi}_z^T \cdot \boldsymbol{T}_e^{n+1} - \tilde{\boldsymbol{\phi}}_z{}^T \cdot \boldsymbol{T}_i^{n+1}\right) + 2\pi \int_{\Omega_\Phi} \cos(\Phi)\left(\boldsymbol{\omega}_\Phi \otimes \frac{\partial \boldsymbol{\psi}_z}{\partial z}\right)^T \cdot \boldsymbol{I}^{n+1}\sin(\Phi)\,\mathrm{d}\Phi \right.$$
$$\left. - \boldsymbol{\phi}_z^T \cdot \boldsymbol{P}_e \right] \mathrm{d}\Omega_z = \mathbf{0}\,.$$

$$a\mathbf{M} \cdot \frac{\boldsymbol{T}_e^{n+1} - \boldsymbol{T}_e^n}{\Delta t} + \mathbf{G}_{ei} \cdot \boldsymbol{T}_e^{n+1} - \tilde{\mathbf{G}}_{ei} \cdot \boldsymbol{T}_i^{n+1} + \mathbf{DI} \cdot \boldsymbol{I}^{n+1} = \boldsymbol{P}_e$$

DG-BGK&Ts scheme, where $\boldsymbol{I}^{n+1} = \mathbf{A} \cdot \boldsymbol{T}_e^{n+1} + \boldsymbol{b}$

$$\mathbf{A}_{T_e}(\mathbf{A}) \cdot \boldsymbol{T}_e^{n+1} + \tilde{\mathbf{G}}_{ei} \cdot \boldsymbol{T}_i^{n+1} = \boldsymbol{b}_{T_e}(\boldsymbol{b})$$

[a]

[a] [Holec et al, IJNMF 83, 779 (2017)]

Approximate multi-group diffusion test

Two energy groups transport model

$$\cos(\Phi)\,\frac{\partial I_{g_j}}{\partial z} = k_{g_j}\left(S_T T - I_{g_j}\right)$$

$$a\,\frac{\partial T}{\partial t} = -\sum_{j=1,2}\frac{2\pi}{\Delta_{g_j}}\int_0^{\pi}\cos(\Phi)\frac{\partial I_{g_j}}{\partial z}\sin(\Phi)\,\mathrm{d}\Phi\ ,$$

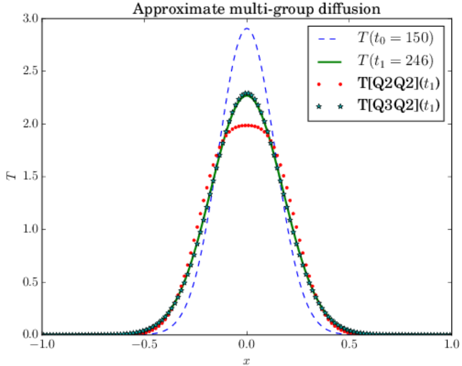

Diffusive(local) asymptotic behavior of the two energy groups transport model

$$I_{g_j} \approx S_T\left(T - \frac{\cos(\Phi)}{k_{g_j}}\frac{\partial T}{\partial z}\right) \xrightarrow{local} a\frac{\partial T}{\partial t} \approx \frac{4\pi S_T}{3}\left(\frac{1}{k_{g_1}\Delta_{g_1}} + \frac{1}{k_{g_2}\Delta_{g_2}}\right)\frac{\partial^2 T}{\partial z^2}\ .$$

cells	32	64	128	256	512
T[Q1Q1]	2.2e-01 [5]	2.4e-01 (-0.1)	2.3e-01 (0.0)	2.3e-01 (0.0)	2.3e-01 (0.0)
T[Q2Q2]	8.7e-02 [4]	9.5e-02 (-0.1)	9.8e-02 (-0.0)	9.6e-02 (0.0)	9.1e-02 (0.1)
T[Q3Q2]	1.2e-01 [4]	5.7e-02 (1.1)	1.0e-02 (2.5)	1.3e-03 (2.9)	–
T[Q3Q3]	7.6e-02 [4]	4.6e-02 (0.7)	9.8e-03 (2.2)	1.3e-03 (2.9)	–
T[Q4Q4]	2.9e-02 [4]	9.6e-03 (1.6)	1.3e-03 (2.9)	–	–
T[Q5Q5]	2.3e-03 [4]	8.2e-05 (4.8)	–	–	–
T[Q6Q6]	1.7e-04 [4]	–	–	–	–

Lagrangian High-Order Curvilinear Framework

$$
\begin{aligned}
\mathbf{M}_{\boldsymbol{v}} \cdot \frac{\mathrm{d}\boldsymbol{v}}{\mathrm{d}t} &= -\mathbf{F} \cdot \mathbf{I} \\
\mathbf{M}_{e} \cdot \frac{\mathrm{d}\boldsymbol{e}}{\mathrm{d}t} &= \mathbf{F}^{T} \cdot \boldsymbol{v} \\
\frac{\mathrm{d}\boldsymbol{x}}{\mathrm{d}t} &= \boldsymbol{v}
\end{aligned}
$$

[Dobrev, Kolev, Rieben, SIAM JSC 34, B606 (2012)]

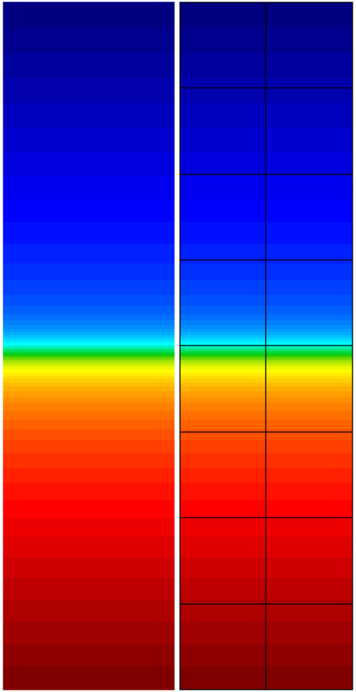

Lagrangian High-Order Curvilinear Framework

$$\mathbf{M}_{\boldsymbol{v}} \cdot \frac{\mathrm{d}\boldsymbol{v}}{\mathrm{d}t} = -\mathbf{F} \cdot \mathbf{I}$$

$$\mathbf{M}_{e} \cdot \frac{\mathrm{d}\boldsymbol{e}}{\mathrm{d}t} = \mathbf{F}^{T} \cdot \boldsymbol{v}$$

$$\frac{\mathrm{d}\boldsymbol{x}}{\mathrm{d}t} = \boldsymbol{v}$$

[Dobrev, Kolev, Rieben, SIAM JSC 34, B606 (2012)]

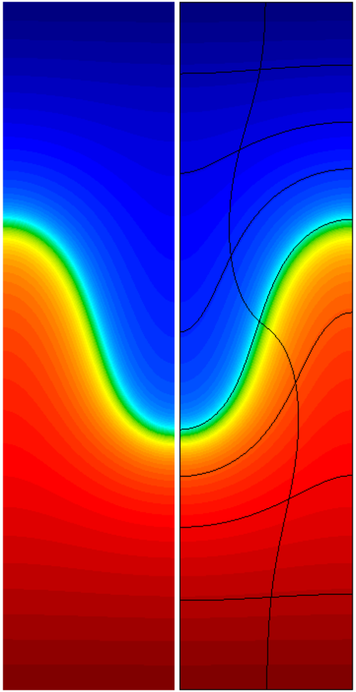

Lagrangian High-Order Curvilinear Framework

$$
\begin{aligned}
\mathbf{M}_{\boldsymbol{v}} \cdot \frac{\mathrm{d}\boldsymbol{v}}{\mathrm{d}t} &= -\mathbf{F} \cdot \mathbf{I} \\
\mathbf{M}_{e} \cdot \frac{\mathrm{d}\boldsymbol{e}}{\mathrm{d}t} &= \mathbf{F}^{T} \cdot \boldsymbol{v} \\
\frac{\mathrm{d}\boldsymbol{x}}{\mathrm{d}t} &= \boldsymbol{v}
\end{aligned}
$$

[Dobrev, Kolev, Rieben, SIAM JSC 34, B606 (2012)]

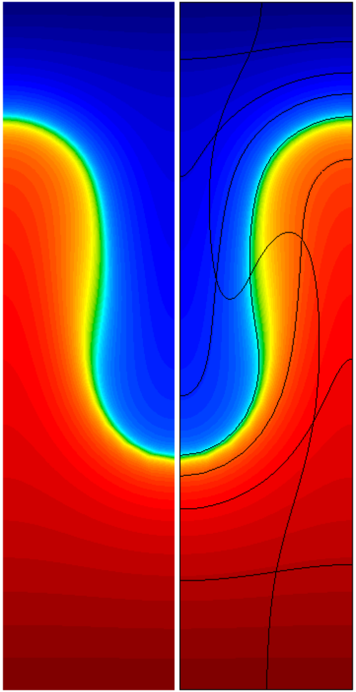

Lagrangian High-Order Curvilinear Framework

$$
\begin{aligned}
\mathbf{M}_{\boldsymbol{v}} \cdot \frac{\mathrm{d}\boldsymbol{v}}{\mathrm{d}t} &= -\mathbf{F} \cdot \mathbf{I} \\
\mathbf{M}_{e} \cdot \frac{\mathrm{d}\boldsymbol{e}}{\mathrm{d}t} &= \mathbf{F}^{T} \cdot \boldsymbol{v} \\
\frac{\mathrm{d}\boldsymbol{x}}{\mathrm{d}t} &= \boldsymbol{v}
\end{aligned}
$$

[Dobrev, Kolev, Rieben, SIAM JSC 34, B606 (2012)]

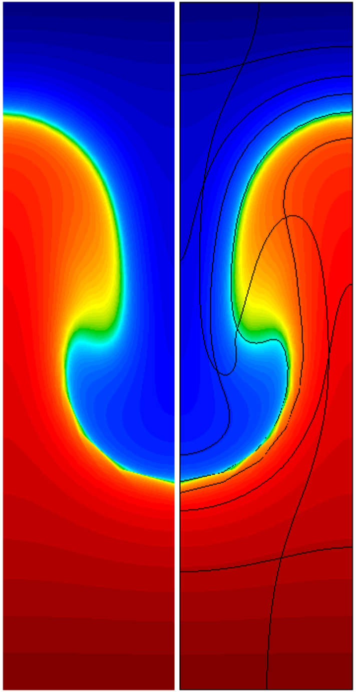

Nonlocal Extension of Lagrangian High-Order Curvilinear Framework

$$\mathbf{M}_{\boldsymbol{v}} \cdot \frac{\mathrm{d}\boldsymbol{v}}{\mathrm{d}t} = -\mathbf{F} \cdot \mathbf{I}$$

$$k_B \mathbf{M}_e \cdot \frac{\mathrm{d}\boldsymbol{T}}{\mathrm{d}t} = \mathbf{F}^T \cdot \boldsymbol{v} - \int_{4\pi} \mathbf{D} \cdot \boldsymbol{I}\, \mathrm{d}\boldsymbol{n}$$

$$\frac{\mathrm{d}\boldsymbol{x}}{\mathrm{d}t} = \boldsymbol{v}$$

$$\mathbf{D} \cdot \boldsymbol{I} = \mathbf{S} \cdot \boldsymbol{T} - ((k+\sigma)\mathbf{M} + \boldsymbol{E} \cdot \mathbf{M}_{\boldsymbol{n}} - \sigma \mathbf{M}\mathbf{I}) \cdot \boldsymbol{I} + \mathbf{B} \cdot \boldsymbol{I} - \tilde{\mathbf{B}} \cdot \tilde{\boldsymbol{I}}$$

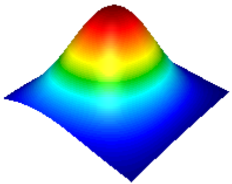

source $\sin(z)\sin(x)$

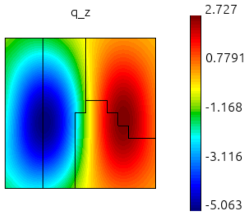

z flux component

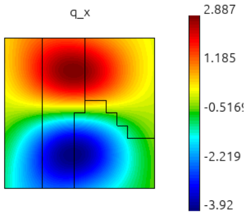

x flux component

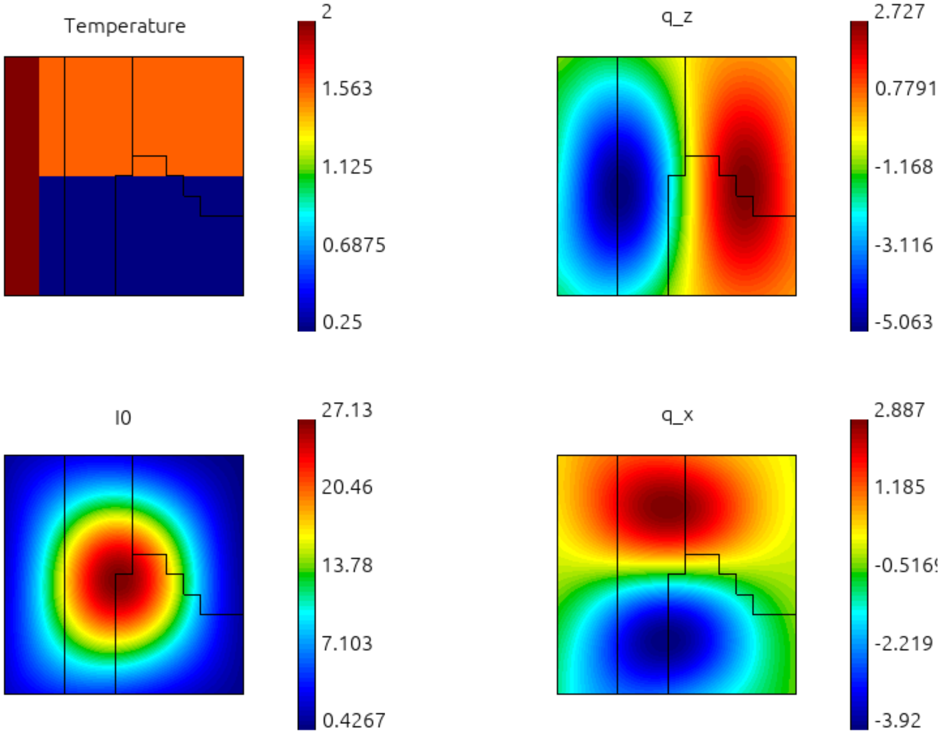
Temperature
2
1.563
1.125
0.6875
0.25
q_z
2.727
0.7791
-1.168
-3.116
-5.063
I0
27.13
20.46
13.78
7.103
0.4267
q_x
2.887
1.185
-2.219
-3.92

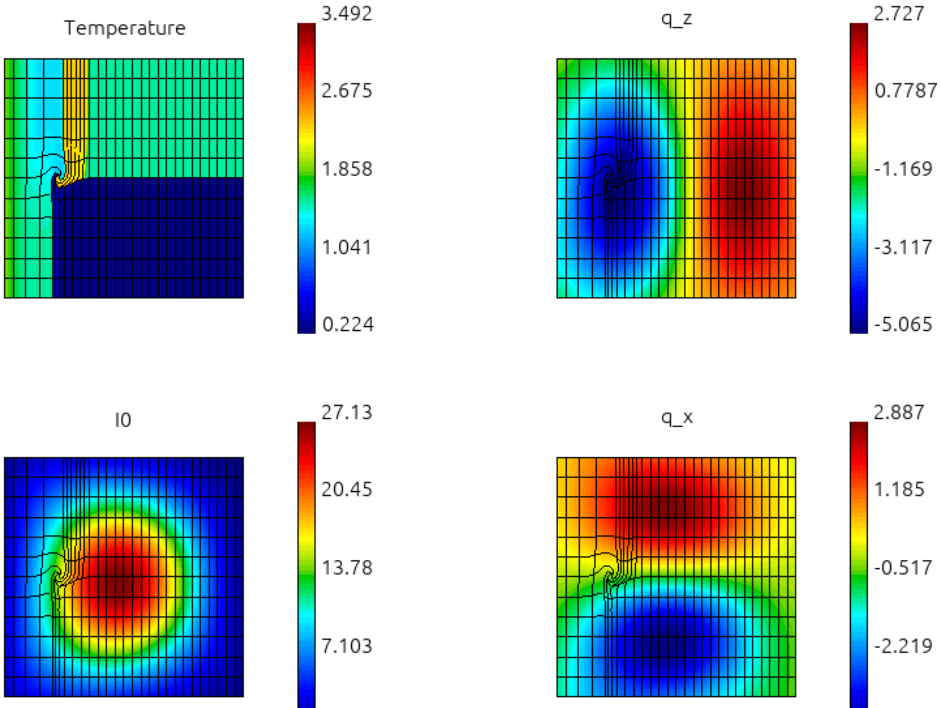

Temperature
3.492
2.675
1.858
1.041
0.224
q_z
2.727
0.7787
-1.169
-3.117
-5.065
I0
27.13
20.45
13.78
7.103
q_x
2.887
1.185
-0.517
-2.219

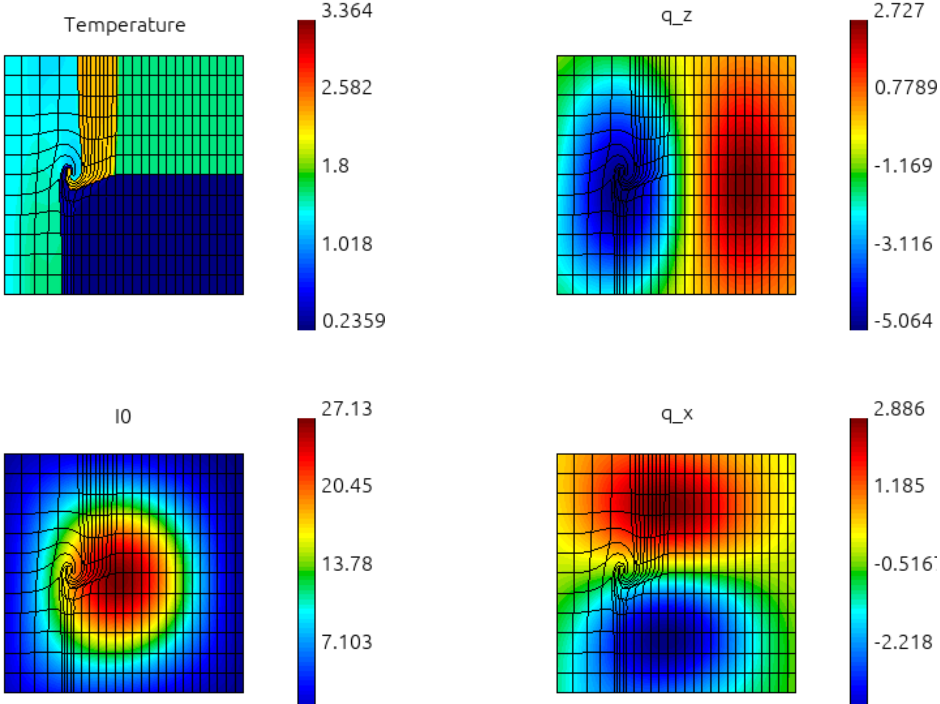
Temperature
3.364
2.582
1.8
1.018
0.2359
q_z
2.727
0.7789
-1.169
-3.116
-5.064
I0
27.13
20.45
13.78
7.103
q_x
2.886
1.185
-0.516
-2.218

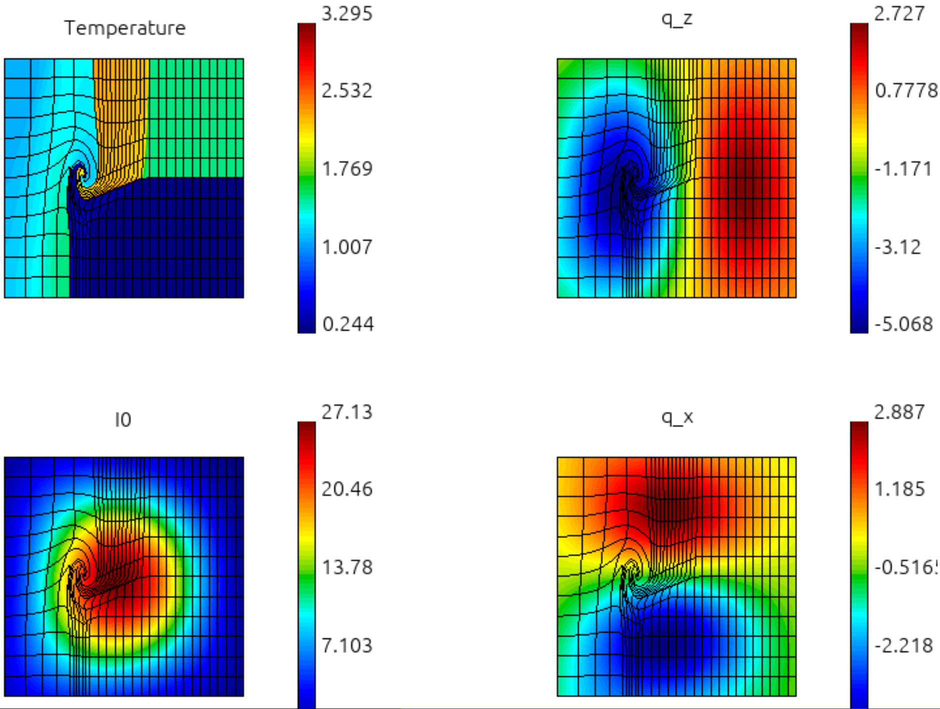
Temperature
3.295
2.532
1.769
1.007
0.244
q_z
2.727
0.7778
-1.171
-3.12
-5.068
I0
27.13
20.46
13.78
7.103
q_x
2.887
1.185
-0.516
-2.218

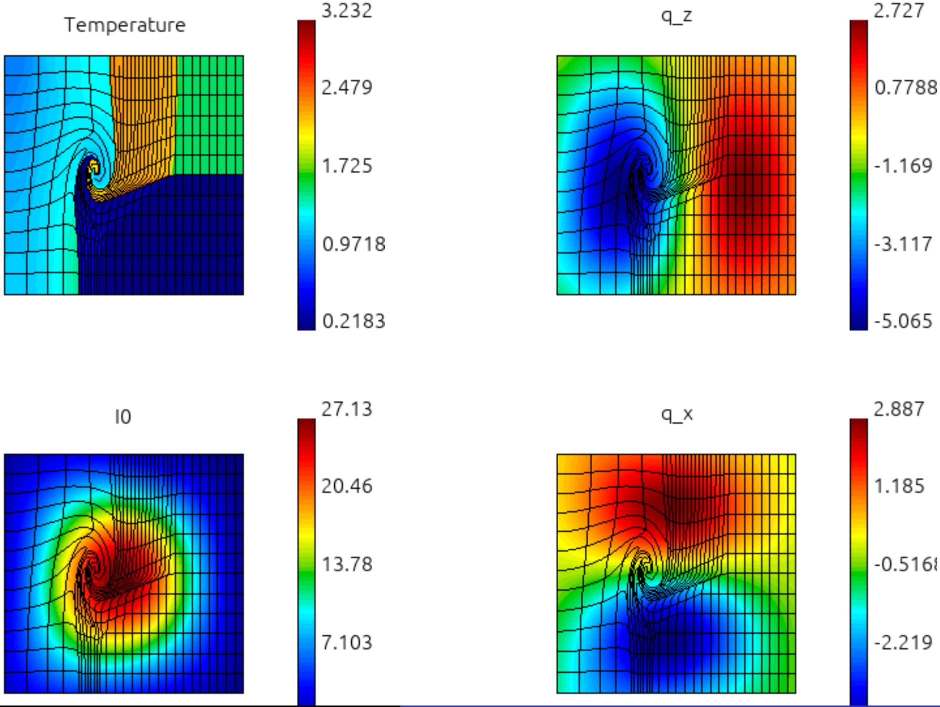
Temperature
3.232
2.479
1.725
0.9718
0.2183
q_z
2.727
0.7788
-1.169
-3.117
-5.065
I0
27.13
20.46
13.78
7.103
q_x
2.887
1.185
-0.516
-2.219

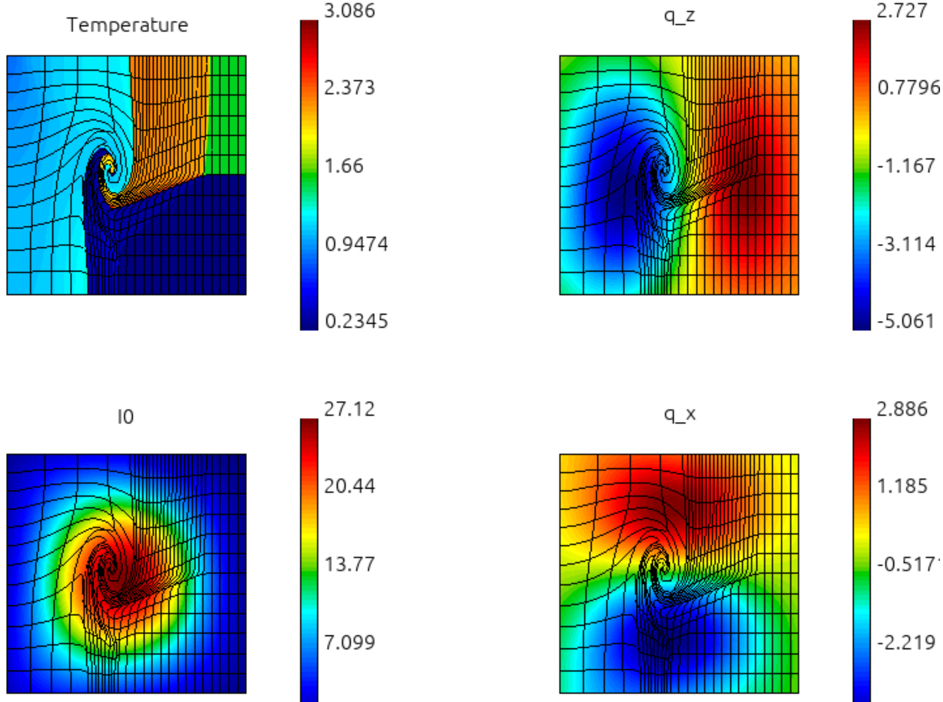
Temperature
3.086
2.373
1.66
0.9474
0.2345
q_z
2.727
0.7796
-1.167
-3.114
-5.061
I0
27.12
20.44
13.77
7.099
q_x
2.886
1.185
-0.517
-2.219

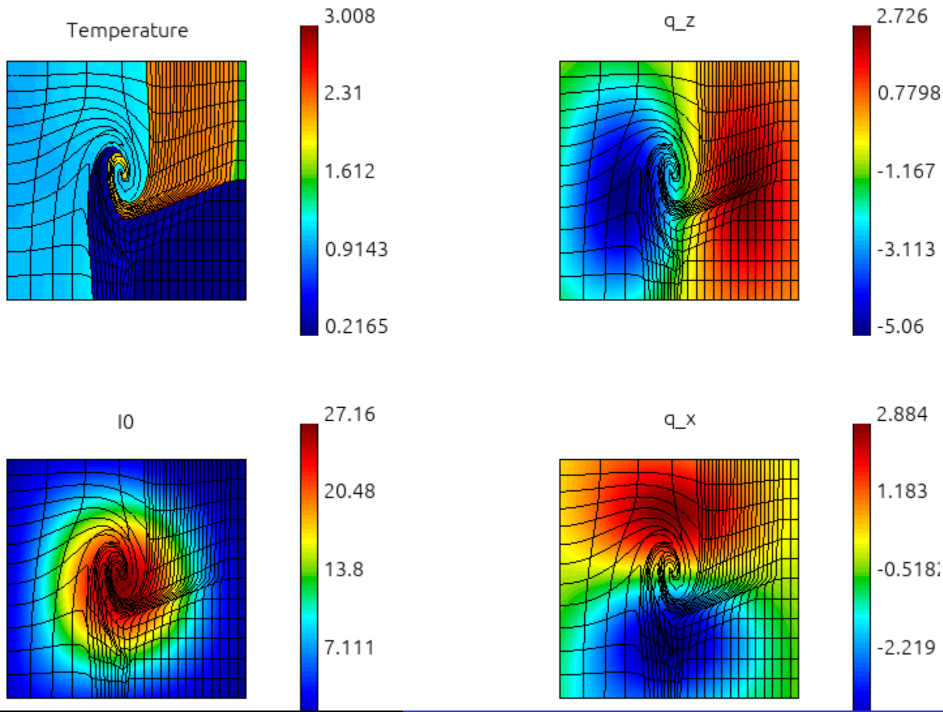
Temperature
3.008
2.31
1.612
0.9143
0.2165
q_z
2.726
0.7798
-1.167
-3.113
-5.06
I0
27.16
20.48
13.8
7.111
q_x
2.884
1.183
-2.219

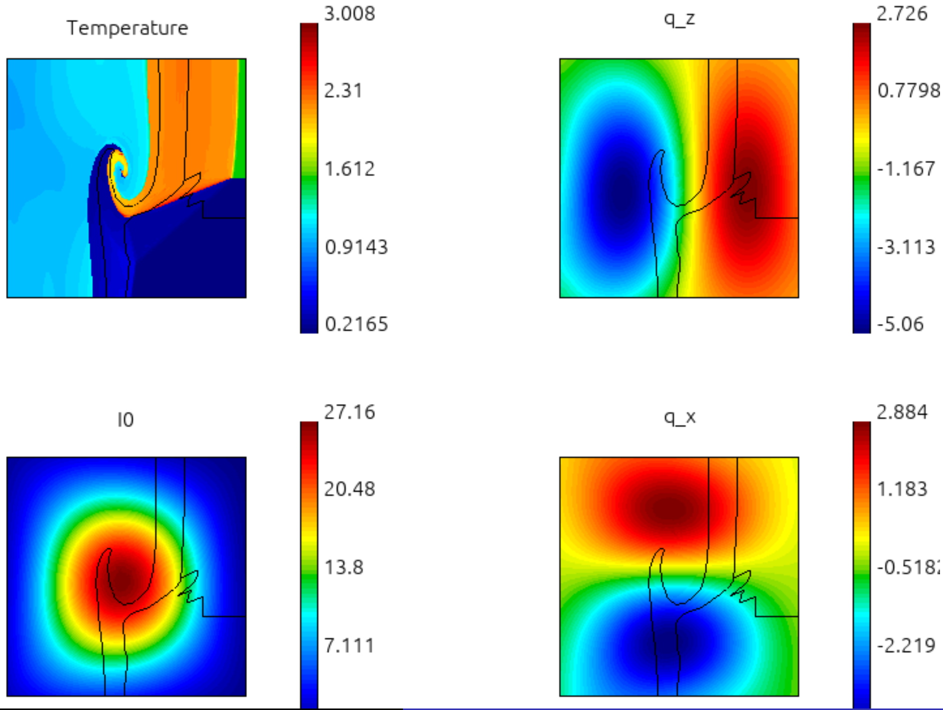
Temperature
3.008
2.31
1.612
0.9143
0.2165
q_z
2.726
0.7798
-1.167
-3.113
-5.06
I0
27.16
20.48
13.8
7.111
q_x
2.884
1.183
-2.219

Curvilinear Framework of Nonlocal Transport

Axisymmetric transport equation

$$
\begin{aligned}
\sin(\phi)\left(\cos(\theta)\frac{\partial I}{\partial r} - \frac{\sin(\theta)}{r}\frac{\partial I}{\partial \theta}\right) + \cos(\phi)\frac{\partial I}{\partial z} &= S_T\, T_e - \left(k + \sigma - \sin(\phi)\cos(\theta)E_r - \cos(\phi)E_z\right) I + \sigma I_0 \\
\mathbf{D}\cdot\boldsymbol{I} &= \mathbf{S}\cdot\boldsymbol{T} - \left((k+\sigma)\mathbf{M} + \boldsymbol{E}\cdot\mathbf{M}_{\boldsymbol{n}} - \sigma\mathbf{MI}\right)\cdot\boldsymbol{I} + \mathbf{B}\cdot\boldsymbol{I} - \tilde{\mathbf{B}}\cdot\tilde{\boldsymbol{I}}
\end{aligned}
$$

[1]

- high-order curvilinear divergence matrix

$$
\begin{aligned}
\mathbf{D} = \int_0^\pi \int_0^\pi \int_\Omega &(\boldsymbol{\omega}_\theta \otimes \boldsymbol{\omega}_\phi \otimes \boldsymbol{\psi}) \otimes \\
&\left(\sin(\phi)\,\boldsymbol{\omega}_\phi \otimes \left(\cos(\theta)\,\boldsymbol{\omega}_\theta^T \otimes \frac{\partial \boldsymbol{\psi}^T}{\partial r} - \frac{\sin(\theta)}{r}\frac{\partial \boldsymbol{\omega}_\theta^T}{\partial \theta} \otimes \boldsymbol{\psi}^T\right) + \boldsymbol{\omega}_\theta^T \otimes \cos(\phi)\,\boldsymbol{\omega}_\phi^T \otimes \frac{\partial \boldsymbol{\psi}^T}{\partial z}\right) r\,\sin(\phi)\mathrm{d}\Omega\mathrm{d}\phi\mathrm{d}\theta
\end{aligned}
$$

- high-order curvilinear numerical flux matrix

$$
\mathbf{B} = \int_0^\pi \int_0^\pi \int_{\Gamma_{\boldsymbol{n}\cdot\boldsymbol{n}_\Gamma < 0}} (\boldsymbol{\omega}_\theta \otimes \boldsymbol{\omega}_\phi \otimes \boldsymbol{\psi}) \otimes (\boldsymbol{\omega}_\theta \otimes \boldsymbol{\omega}_\phi \otimes \boldsymbol{\psi})^T \left(\sin(\phi)\cos(\theta)n_{\Gamma_r} + \cos(\phi)n_{\Gamma_z}\right) r\,\sin(\phi)\mathrm{d}\Gamma\mathrm{d}\phi\mathrm{d}\theta
$$

- proper treatment of Lorentz force

$$
\boldsymbol{E}\cdot\boldsymbol{n}\frac{\partial I}{\partial|\boldsymbol{v}|} + (\boldsymbol{E} + \boldsymbol{n}\times\boldsymbol{B})\cdot\nabla_{\boldsymbol{n}} I = \begin{bmatrix} E_x \\ E_y \\ E_z \end{bmatrix}^T \cdot \begin{bmatrix} \cos(\theta)\sin(\phi) \\ \sin(\theta)\sin(\phi) \\ \cos(\phi) \end{bmatrix} \frac{\partial I}{\partial|\boldsymbol{v}|} + \left(\begin{bmatrix} E_x \\ E_y \\ E_z \end{bmatrix} + \begin{bmatrix} \cos(\theta)\sin(\phi) \\ \sin(\theta)\sin(\phi) \\ \cos(\phi) \end{bmatrix} \times \begin{bmatrix} B_x \\ B_y \\ B_z \end{bmatrix}\right)^T \cdot \begin{bmatrix} \cos(\phi)\frac{\partial I}{\partial \phi} \\ \frac{1}{\sin(\phi)}\frac{\partial I}{\partial \theta} \\ -\sin(\phi)\frac{\partial I}{\partial \phi} \end{bmatrix}
$$

[1] mfem.org – "My finite element library is higher order than yours..."

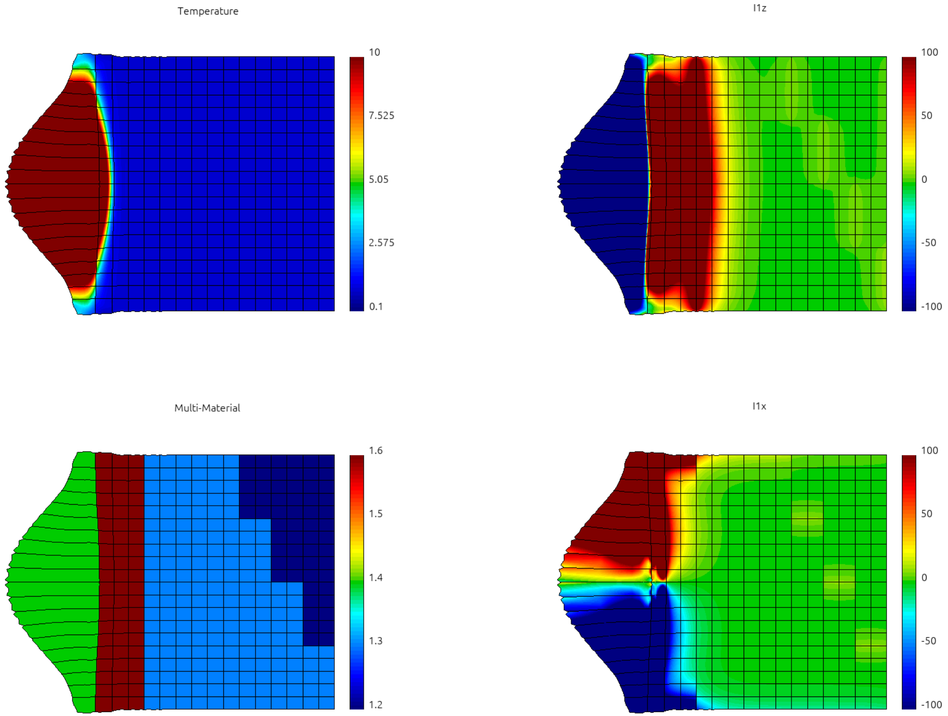
Temperature
10
7.525
5.05
2.575
0.1
I1z
100
50
0
-50
-100
Multi-Material
1.6
1.5
1.4
1.3
1.2
I1x
100
50
0
-50
-100

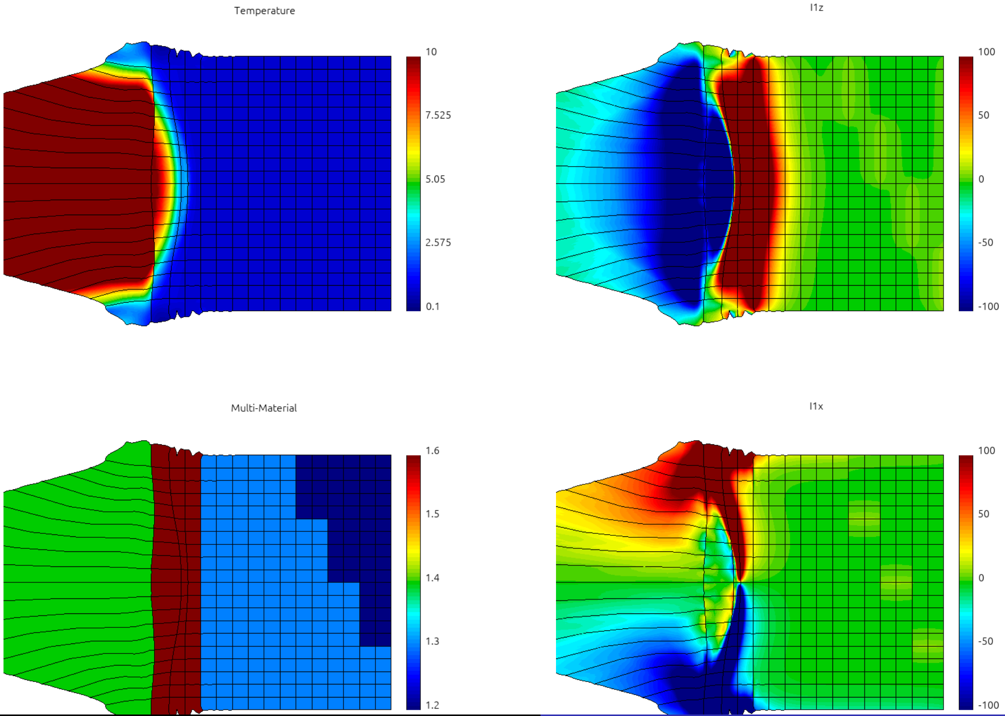
Temperature
10
7.525
5.05
2.575
0.1
l1z
100
50
0
-50
-100
Multi-Material
1.6
1.5
1.4
1.3
1.2
l1x
100
50
0
-50
-100

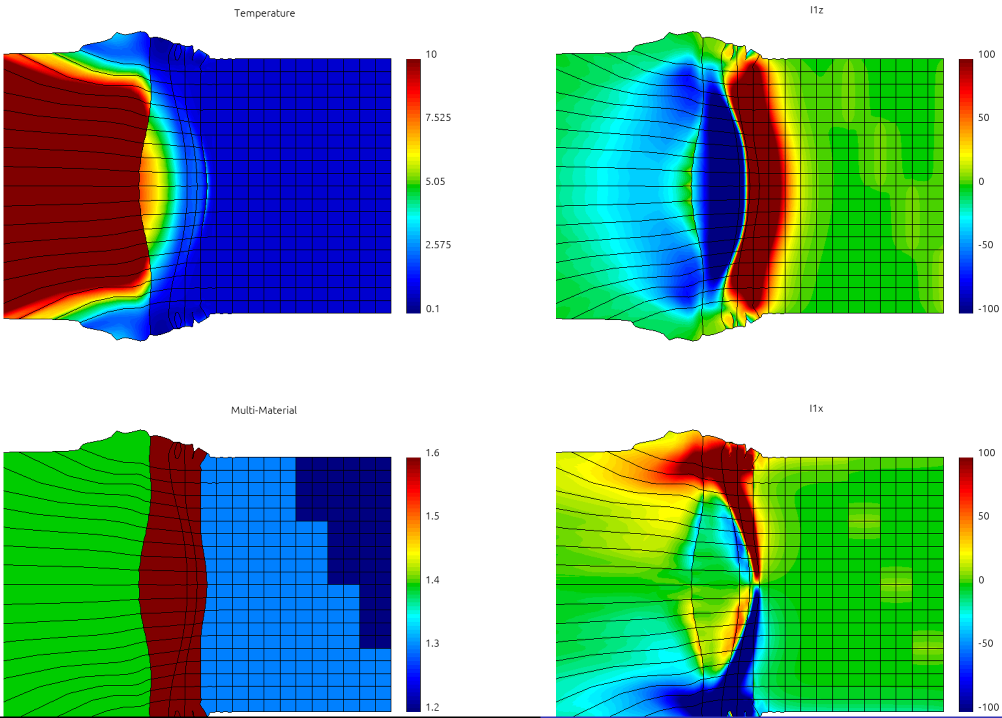
Temperature
10
7.525
5.05
2.575
0.1
I1z
100
50
0
-50
-100
Multi-Material
1.6
1.5
1.4
1.3
1.2
I1x
100
50
0
-50
-100

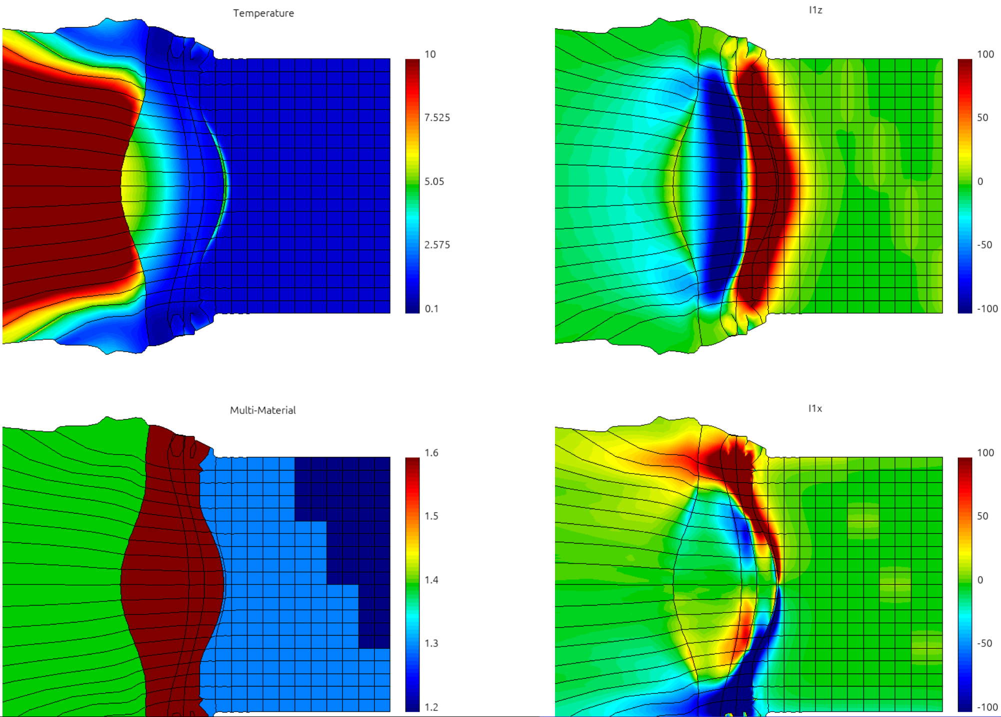
Temperature
10
7.525
5.05
2.575
0.1
I1z
100
50
0
-50
-100
Multi-Material
1.6
1.5
1.4
1.3
1.2
I1x
100
50
0
-50
-100

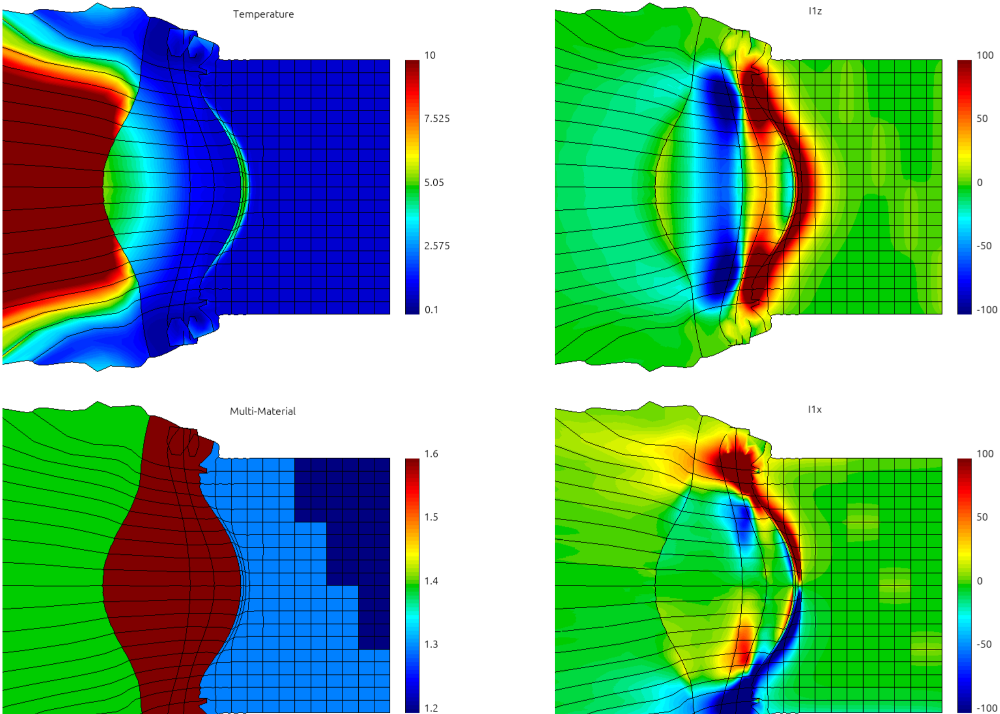
Temperature
10
7.525
5.05
2.575
0.1
I1z
100
50
0
-50
-100
Multi-Material
1.6
1.5
1.4
1.3
1.2
I1x
100
50
0
-50
-100

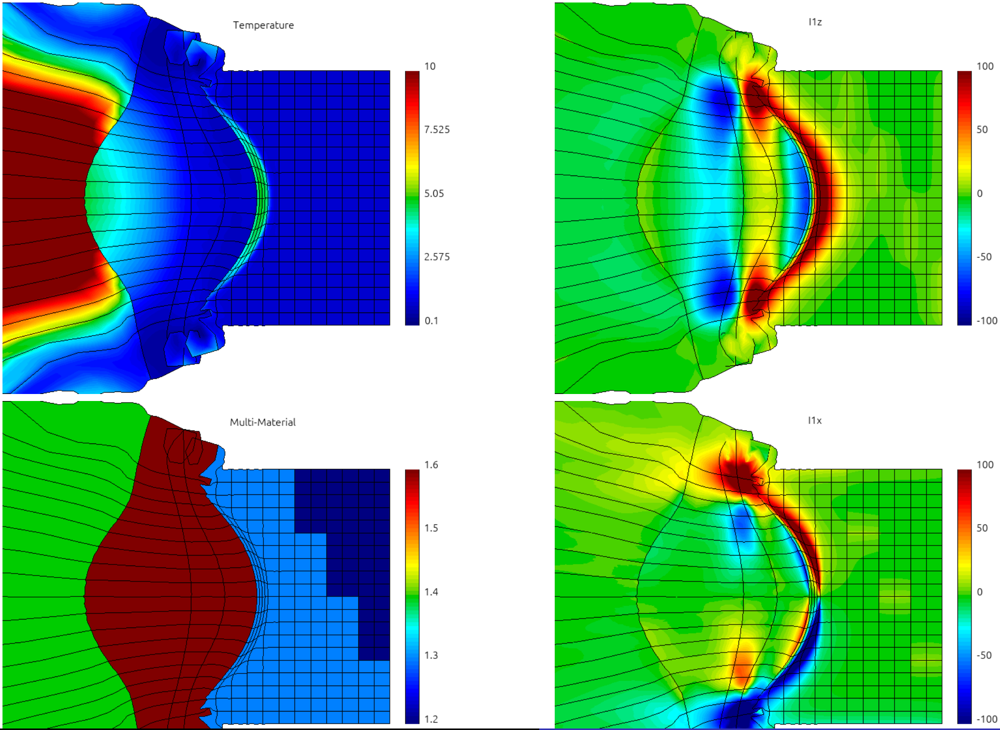
Temperature
10
7.525
5.05
2.575
0.1
I1z
100
50
0
-50
-100
Multi-Material
1.6
1.5
1.4
1.3
1.2
I1x
100
50
0
-50
-100

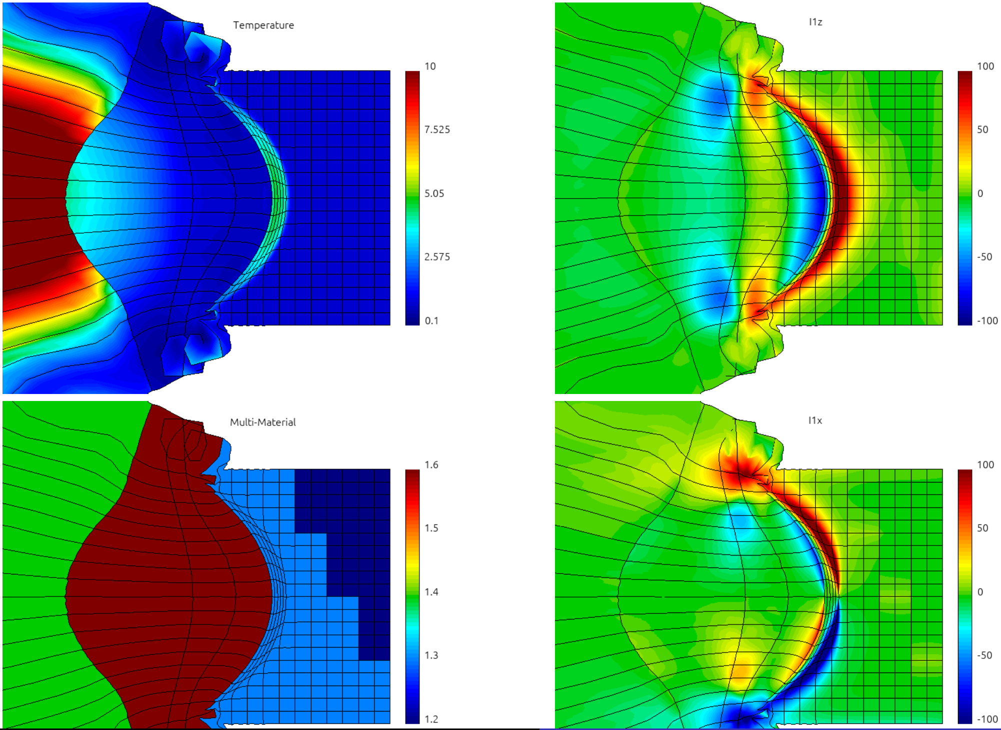
Temperature
10
7.525
5.05
2.575
0.1
I1z
100
50
0
-50
-100
Multi-Material
1.6
1.5
1.4
1.3
1.2
I1x
100
50
0
-50
-100

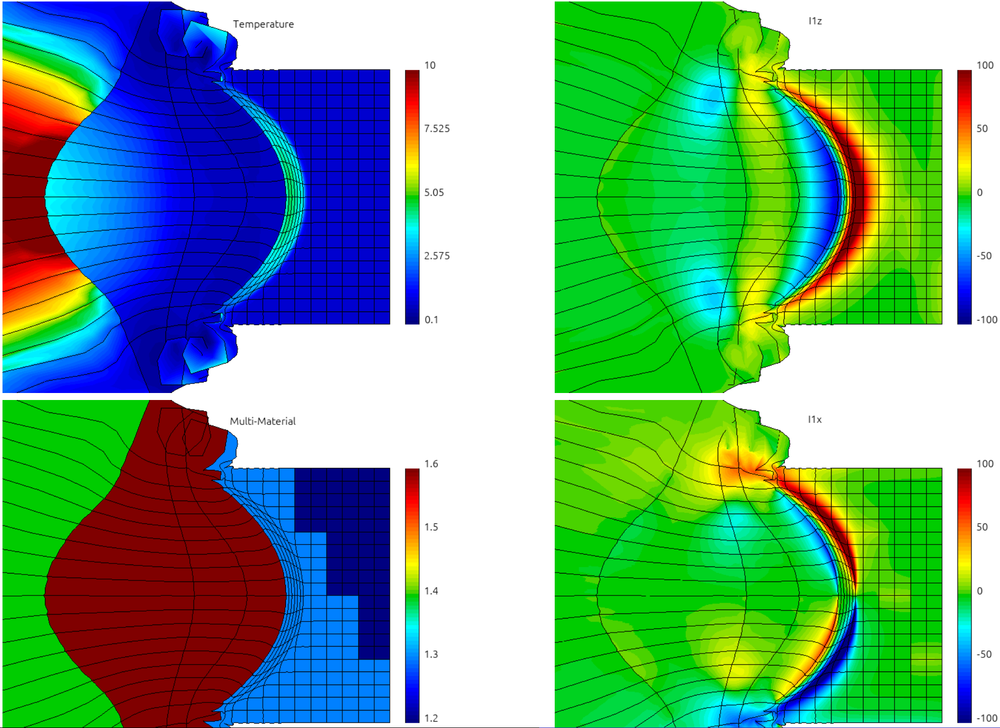
Temperature
10
7.525
5.05
2.575
0.1
I1z
100
50
0
-50
-100
Multi-Material
1.6
1.5
1.4
1.3
1.2
I1x
100
50
0
-50
-100

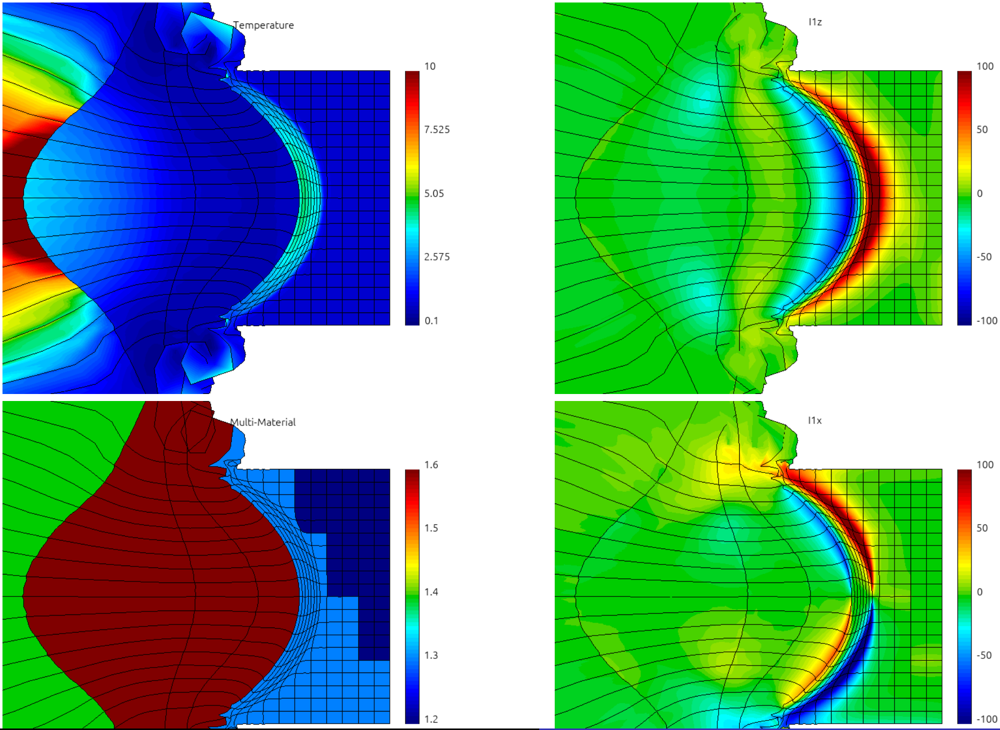
Temperature
10
7.525
5.05
2.575
0.1
I1z
100
50
0
-50
-100
Multi-Material
1.6
1.5
1.4
1.3
1.2
I1x
100
50
0
-50
-100

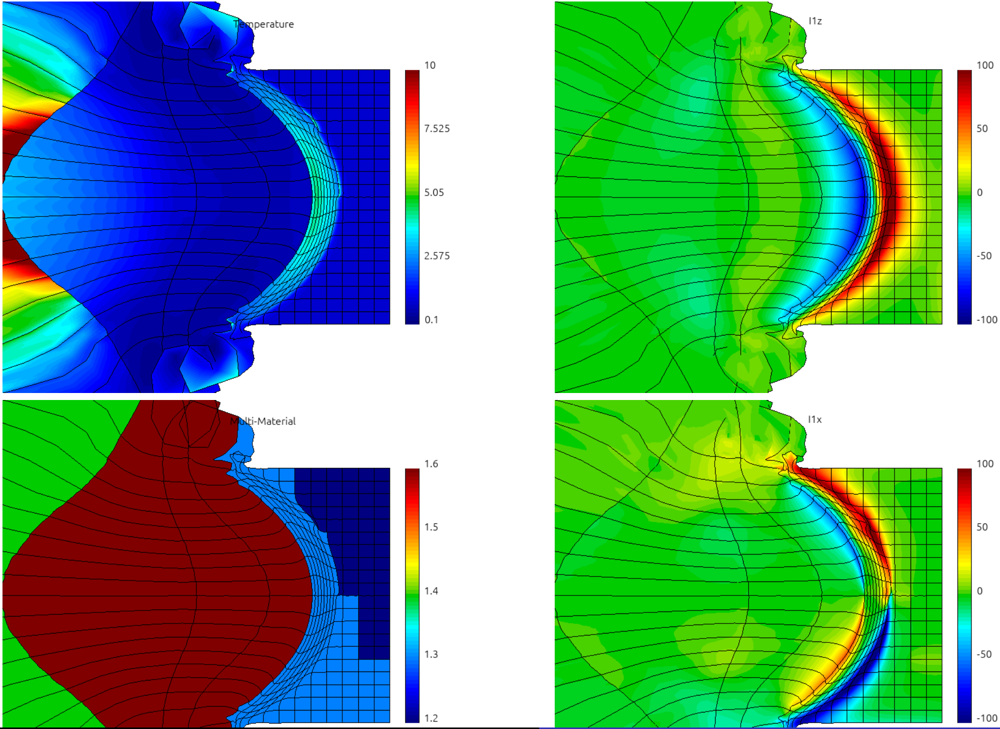
Temperature
10
7.525
5.05
2.575
0.1
I1z
100
50
0
-50
-100
Multi-Material
1.6
1.5
1.4
1.3
1.2
I1x
100
50
0
-50
-100

Preheat observed in a shocked CH foam at Omega

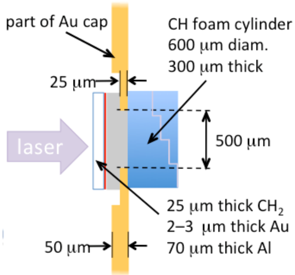

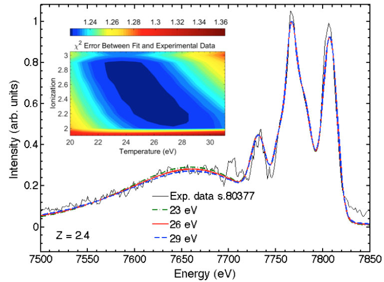

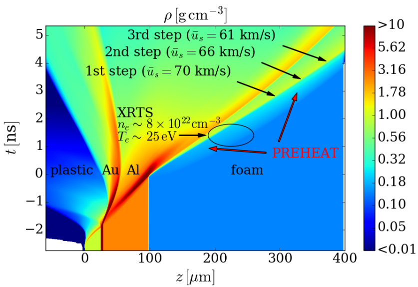

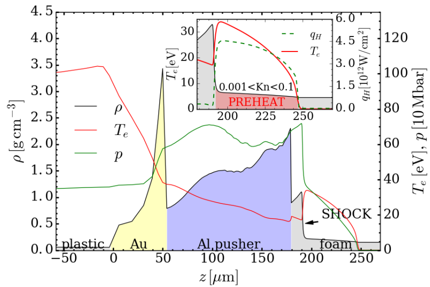

flat 2 ns laser pulse, 8×10^{14} Wcm2, 300 μm thick foam ($\rho = 0.13$ g/cm^3)

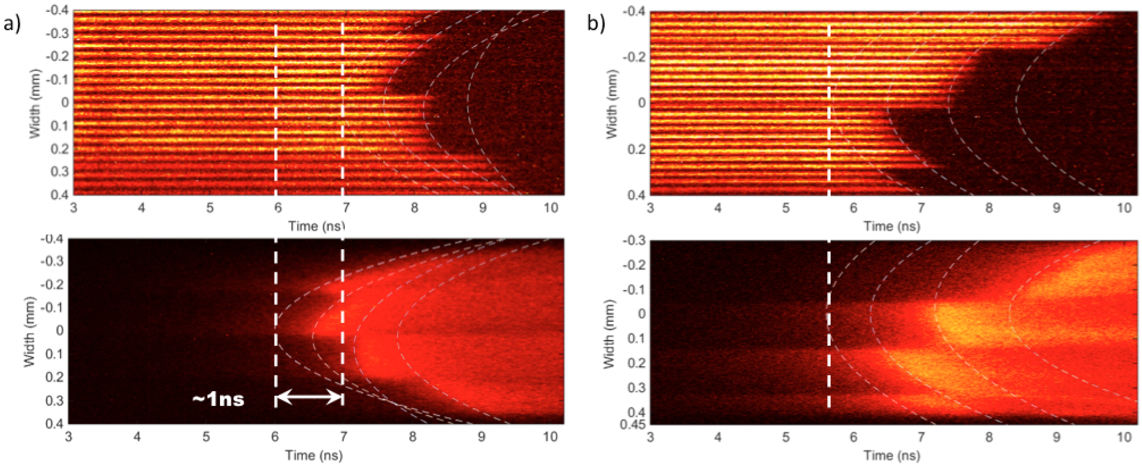

a) recent experiment with new phase-plates, b) previous experiment

Rankine-Hugoniot jump condition analysis

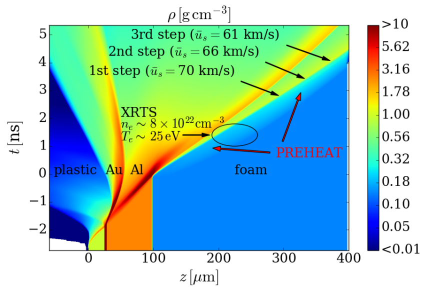

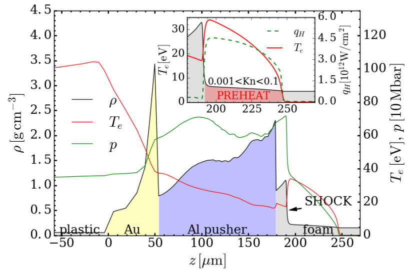

$$
\begin{aligned}
u_s(\rho_0 - \rho_1) &= \rho_0 u_0 - \rho_1 u_1 \\
u_s(\rho_0 u_0 - \rho_1 u_1) &= (\rho_0 u_0^2 + p_0) - (\rho_1 u_1^2 + p_1) \\
u_s(E_0 - E_1) &= u_0(E_0 + p_0) - u_1(E_1 + p_1) + (q_{e0} + q_{R0}) - (q_{e1} + q_{R1})
\end{aligned}
$$

Rankine-Hugoniot jump condition of energy

$$u_s = \frac{\Delta q_{tot}}{\Delta E} = \frac{u_0(E_0 + p_0) - u_1(E_1 + p_1) + (q_{e0} + q_{R0}) - (q_{e1} + q_{R1})}{E_0 - E_1}$$

The high shock velocity 70 km/s is because the electron flux contribution
$q_{e1} - q_{e0} \approx -2(p_1 u_1 - p_0 u_0) \approx 0.16(u_1(E_1 + p_1) - u_0(E_0 + p_0))$,
which is comparable to the hydrodynamics flux contribution.

Nonlocal vs. SH diffusion

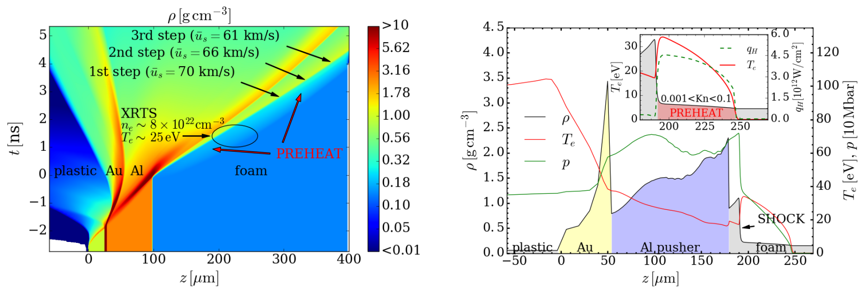

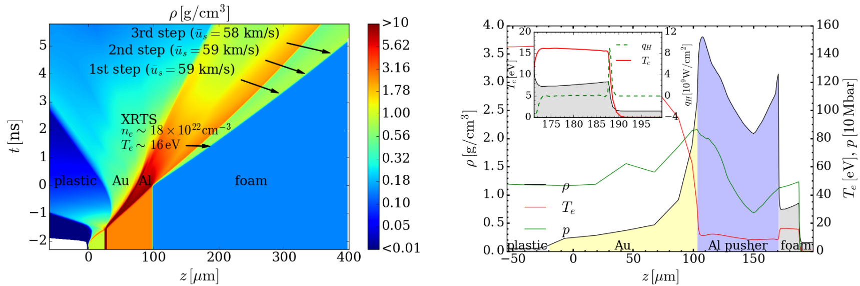

Effective mean free path was $4.1 \times v_T$, according to LANL code ATOMIC the mean free path in WDM foam increases $\approx 30\%$.

X-ray preheat analysis

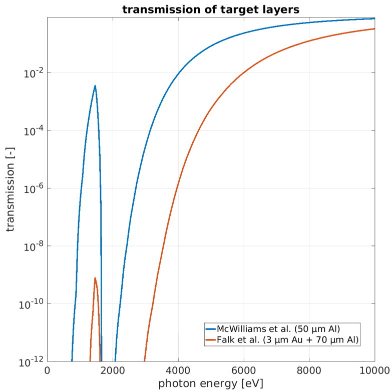

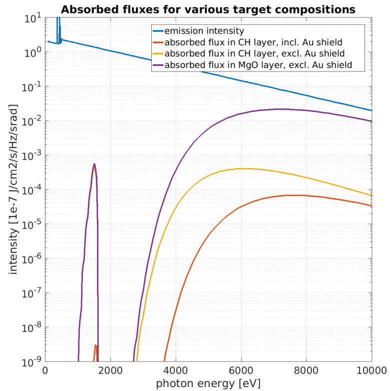

Significant part of x-rays $<$ 2keV (penetration depth is small) $\rightarrow$ energy absrobed in the surface of the foam is $\approx$ 670 J/cm3.
Absorbed energy density by nonlocal electrons $\approx$ 2.7e6 J/cm3.

Conclusions

Plasma Euler and Transport Equations hydro code PETE

$$\frac{\partial \rho}{\partial t} = -\nabla \cdot (\rho \boldsymbol{u}),$$

$$\frac{\partial \rho \boldsymbol{u}}{\partial t} = -\nabla \cdot (\rho \boldsymbol{u} \otimes \boldsymbol{u} + p\mathbf{I}),$$

$$\frac{\partial E}{\partial t} = -\nabla \cdot (E\boldsymbol{u} + p\boldsymbol{u} + \boldsymbol{q}_L + \boldsymbol{q}_e + \boldsymbol{q}_R),$$

density ρ, fluid velocity $\boldsymbol{u}$, total energy $E(T)$, pressure $p(\rho, T)$, laser energy flux $\boldsymbol{q}_L$, electron heat flux $\boldsymbol{q}_e$, radiation flux $\boldsymbol{q}_R$.

$$\boldsymbol{n} \cdot \nabla I^p = \frac{\sigma^p T_e - I^p}{\lambda^p},$$

$$\boldsymbol{q}_R = \int_{4\pi} \boldsymbol{n}\, I^p \, \mathrm{d}\boldsymbol{n},$$

$$\boldsymbol{n} \cdot \nabla I^e = \frac{\sigma^e T_e - I^e}{\lambda^e},$$

$$\boldsymbol{q}_e = \int_{4\pi} \boldsymbol{n}\, I^e \, \mathrm{d}\boldsymbol{n},$$

- Lagrangian frame, 2T single fluid, IB laser deposition, SESAME
- Nonlocal radiation and electron transport
- Inherent coupling of nonlocal transport and energy equations via $I = a(\boldsymbol{x}, \boldsymbol{n})\, T_e + b(\boldsymbol{x}, \boldsymbol{n})$, which leads to a temperature dependence of energy fluxes $\boldsymbol{q}_e + \boldsymbol{q}_R = \mathbf{A}\, T_e + \boldsymbol{b}$
- Extension of PETE to 2D Cartesian/axisymmetric based on HONTS and Laghos soon

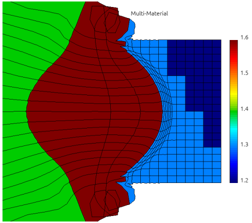

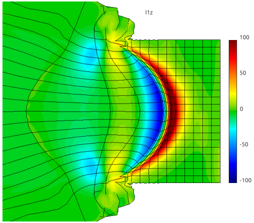

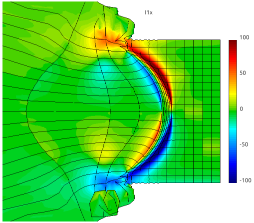

Nonlocal Transport Magneto-Hydrodynamics (NTMHD) model

$$\boldsymbol{n}\cdot\nabla_x f + \frac{q_e}{m_e|\boldsymbol{v}|}\left(\boldsymbol{E}\cdot\boldsymbol{n}\frac{\partial}{\partial|\boldsymbol{v}|}f + \left(\frac{\boldsymbol{E}}{|\boldsymbol{v}|} + \frac{\boldsymbol{n}}{c}\times\boldsymbol{B}\right)\cdot\nabla_{\boldsymbol{n}} f\right) = \frac{f_{MB}(|\boldsymbol{v}|, T_e) - f}{\lambda_{ei}(|\boldsymbol{v}|^4)}$$

NTH Electric field vs. generalized Ohm's law

$$\sum_g \int_{\Delta v^g} \frac{e}{m_e v}\left(\frac{1}{v}\frac{\partial}{\partial v}\left(v^2 \boldsymbol{f}_2\right) + (\boldsymbol{f}_2 - f_0\mathbf{I})\right)\mathrm{d}v\cdot\boldsymbol{E} = \sum_g \int_{\Delta v^g} v\nabla\cdot\boldsymbol{f}_2 + (\nu_{ee} + \nu_{tot})\boldsymbol{f}_1\mathrm{d}v + \sum_g \int_{\Delta v^g} \frac{e}{m_e c}\boldsymbol{f}_1\mathrm{d}v\times\boldsymbol{B}$$

$$\boldsymbol{E} = \frac{1}{en_e}(\boldsymbol{R}_T - \nabla p_e) + \frac{\boldsymbol{j}}{en_e\sigma} + \frac{1}{en_e c}\boldsymbol{j}\times\boldsymbol{B}$$

$$\nabla\times\boldsymbol{E} = -\frac{1}{c}\frac{\partial\boldsymbol{B}}{\partial t} \qquad \text{(life of magnetic field}\boldsymbol{B}\text{)}$$

$$\nabla\times\boldsymbol{B} = \frac{4\pi}{c}\left(\boldsymbol{j}+\tilde{\boldsymbol{j}}\right) \qquad \left(\text{quasi-neutrality}\nabla\cdot\left(\boldsymbol{j}+\tilde{\boldsymbol{j}}\right) = 0\right)$$

Applying generalized Ohm's and Ampere's laws, we get

$$\nabla\times\boldsymbol{E} = \nabla\times\left(\frac{1}{en_e}(\boldsymbol{R}_T - \nabla p_e) + \frac{c}{en_e\sigma 4\pi}\nabla\times\boldsymbol{B} - \frac{\tilde{\boldsymbol{j}}}{en_e\sigma} + \frac{1}{en_e c}\boldsymbol{j}\times\boldsymbol{B}\right)$$

Maxwell Equations for Hydrodynamics - dynamo equation for nonlocal magnetic field source

$$\frac{1}{c}\frac{\partial\boldsymbol{B}}{\partial t} = -\nabla\times\frac{1}{en_e c}\boldsymbol{j}\times\boldsymbol{B} - \nabla\times\frac{c}{en_e\sigma 4\pi}\nabla\times\boldsymbol{B} - \nabla\times\left(\frac{\sum_g\int_{\Delta v^g} v\nabla\cdot\boldsymbol{f}_2\mathrm{d}v}{\sum_g\int_{\Delta v^g}\frac{e}{m_e v}\left(\frac{1}{v}\frac{\partial}{\partial v}\left(v^2\boldsymbol{f}_2\right) + (\boldsymbol{f}_2 - f_0\mathbf{I})\right)\mathrm{d}v} + -\frac{\tilde{\boldsymbol{j}}}{en_e\sigma}\right)$$

Vlasov-Fokker-Planck simulations

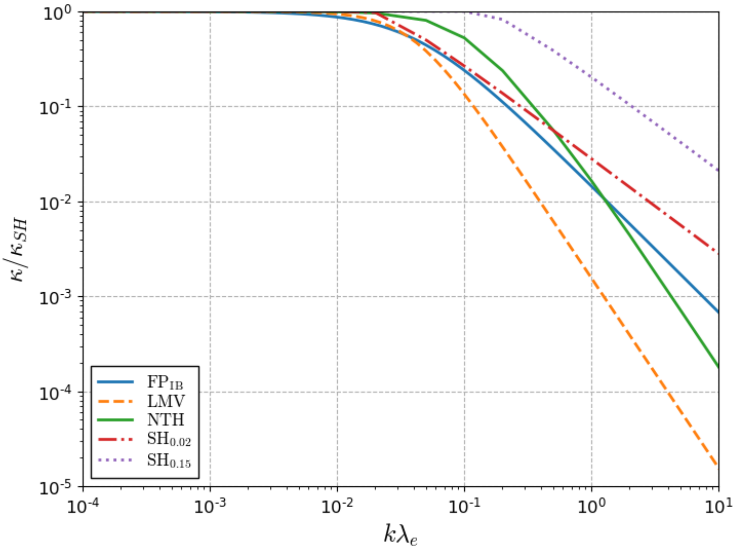

3

[3] Kinetic simulations provided by Jan Nikl (ELI Beamlines).

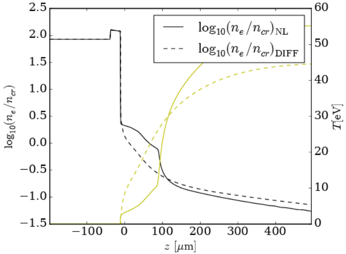

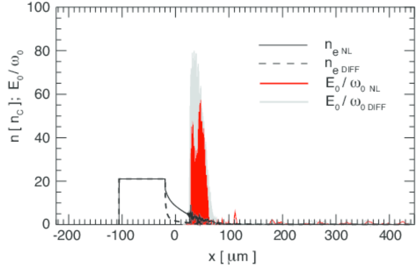

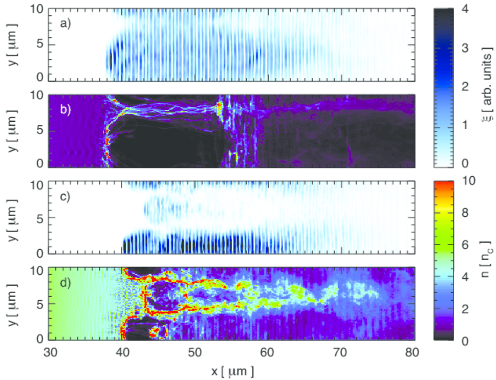

4

[4] OSIRIS PIC simulations by Marija Vranic 2017.